Hindawi
Geofluids
Volume 2022, Article ID 4358328, 11 pages
https://doi.org/10.1155/2022/4358328

Research Article

Effect of Pore Geometry on Nanoconfined Bulk-Gas Flow Behavior

Yi Zhang

College of Biology and Agriculture (College of Food Science and Technology), Zunyi Normal University, 563006, China

Correspondence should be addressed to Yi Zhang; sciyiyi@126.com

Received 15 March 2022; Revised 1 April 2022; Accepted 7 April 2022; Published 27 April 2022

Academic Editor: Zheng Sun

In order to improve energy consumption structure in Guizhou province, China, the efficient development of shale gas becomes more and more important. However, the theoretical understanding, towards microscopic gas flow mechanism, is still weak and insufficient. Although many models have been established, one part of them fails to cover all flow mechanisms, and the other part contains several fitting parameters. Moreover, nanopores can be divided into circular pore and slit pore in accordance with pore geometry. For cylindrical nanopores, by fully comparing with the existed models, a new bulk-gas transport model is proposed by weight superposition of slip flow and Knudsen diffusion, in which weight factors are obtained by Wu's model and Knudsen's model, respectively. For slit pores, an analytical equation for bulk-gas flow is proposed as well, which is free of any fitting parameters. The reliability of the proposed models has been clarified. The impacts of reservoir pressure, pore scale, and gas flow mechanism on bulk-gas flow behavior in process of shale gas development are analyzed. It is found that gas transport capacity of slit nanopores is significantly higher than that of cylindrical nanopores at the same pore scale. For slit nanopores, the larger the aspect ratio, the stronger bulk-gas transmission capacity. As the established models are free of fitting parameters and can be applied into the entire Kn range with sufficient accuracy, the research will greatly benefit shale gas development.

1. Introduction

In Guizhou province, China, shale gas is an emerging unconventional natural gas resource, and its development has the potential to reduce local coal combustion. Unlike conventional oil/gas reservoirs, pore size in shale rock is fairly small, falling in the nanoscale, which leads to the inapplicability of the traditional Navier-Stocks equation to describe gas flow behavior. Gas transmission characteristics in nanopores have attracted more and more attention [1, 2]. Karacan and Siriwardane et al. reported that the diameter of matrix pores is less than 10 nm, several times molecular diameter [3, 4]. Howard shows that the pore radius of Frio shale falls in the 5~15 nm range [5]. Nelson experimentally measured that the minimum pore radius in shale is about 5 nm and the maximum pore radius is about 100 nm [6]. In nanoscale, the gas velocity on the pore wall is no longer zero, and the classical Navier-Stokes equation cannot describe the bulk-gas transmission capacity [7–9]. Establishment of a model, suitable for characterizing the gas transmission characteristics in nanopores, will greatly enhance the prediction accuracy of shale gas production performance.

Up to now, the methods, used to describe the bulk-gas transport capacity in nanopores, can be divided into two categories, including molecular simulation as well as analytical equation. Molecular simulation mainly includes lattice Boltzmann [10], direct Monte Carlo [11, 12], and molecular dynamic simulation [13, 14]. MD method calculates the position, energy, and state of each molecules across the whole simulation time, which can accurately simulate the gas transmission characteristics in nanopores. While a single simulation case requires huge computing resources, moreover the simulation timespan is very short, usually less than nanosecond, which fails to meet the realistic physical process in shale [15–17]. In contrast, the analytical model has the advantages of simple calculation and strong practicability, and it can analyze the characteristics of bulk-gas transmission in extreme cases. It may reveal phenomena that are difficult to be simulated by molecular simulation and experiment. Meanwhile, its deficiency is the limited scope of application. Although many analytical models have been established, some of them do not cover all flow mechanisms, the other part contains several fitting parameters, which often have a great impact on the accuracy of the model.

In 1937, Adzumi studied the flow characteristics of gas in capillary by a large number of experiments and proposed that the determination of fluid flow mechanism depends on Knudsen number. Based on this, the flow mechanism is divided into viscous flow, transition flow, and Knudsen diffusion and developed a full-Kn model by weight superposition of viscous flow and Knudsen diffusion. Unfortunately, Adzumi did not give the specific expression of the weight factor [18–20]. Liu et al. [21] gave the specific expression of the weight factor, but the established bulk-gas transmission model is limited to the case when the Knudsen number is less than 1. Ertekin et al. [22] refer to the existing concept of weight factor to couple Knudsen diffusion and Fick diffusion, but the weight factor will not change with Knudsen number, which quite conflicts with simulation results and experimental data. Azom and Javadpour and Singh and Javadpour [23, 24] linearly added slippage flow and Knudsen diffusion and obtained the full Knudsen number transmission model, but it contains a fitting parameter. Based on the basic theory proposed by Adzumi, Agulera et al. [25] give the weight coefficient, but it also contains three fitting parameters. Beskok and Karniadakis [26] corrected the slippage flow by introducing the molecular sparsity coefficient and extended the formula to the full Knudsen range, but the model contains three fitting parameters. The model proposed by Wu and Xiangfang [27] is based on Beskok's model and takes the intermolecular collision frequency and the collision frequency between molecules and wall as the weight coefficient, including three fitting parameters. Rahmanian et al. [28] referred to the empirical coefficient proposed by Agulera and gave a gas transport model suitable for nanopores with different cross sections, while it includes three fitting parameters. Comparing the established models with the molecular simulation results, it is found that most of the models suffer low accuracy, especially for the slippage flow and transition flow stage.

Because the minerals, forming shale rock, are different in chemical composition, lattice structure, particle size, and petrophysical properties, as a result, the type and size of the formed intergranular, interlayer, and intergranular pores are also different [29–31]. In this paper, the nanopores in the reservoir are simplified into two types, including cylindrical pores and slit pores. As for circular pores, by fully comparing the existed bulk-gas transport models and analyzing their advantages and disadvantages [14, 32], the weight factors of molecular free diffusion and slippage flow are derived, respectively, by referring to Knudsen's model and Wu's model. For slit nanopores, based on the proposed model for cylindrical nanopores, an analytical model of bulk-gas transmission is established for the first time by modifying the corresponding weight factor coefficients. The established bulk-gas transport models do not contain fitting parameters and are suitable for the full Knudsen number range. On this basis, the effects of pore morphology, pore scale, and reservoir pressure on gas bulk phase transmission capacity are studied, and the variation characteristics of bulk-gas transmission capacity in different development stages of shale gas are quantitatively analyzed.

2. Nanoconfined Bulk-Gas Flow Mechanism with Different Pore Geometry

Knudsen number is defined as the ratio of the free path of gas molecules to representative pore size of porous media, characterizing the rarefaction effect of gas [33]. Then, based on the Knudsen number, Schaaf divides the bulk-gas transport mechanism into four basic types [34], namely, continuous flow, slippage flow, transition flow, and Knudsen diffusion. Among them, continuous flow, slippage flow, and Knudsen diffusion had formed a relatively complete theoretical system after years of research. However, accurate description upon the characteristics of transition flow is still challenging.

$$Kn = \frac{\lambda}{d}, \tag{1}$$

where λ is the average free path of gas molecules, m; d is the pore diameter, m.

Taking methane as an example, the molecular effective radius is 0.4 nm. The variation relationship of the average molecular free path with reservoir pressure and temperature is given below.

$$\lambda = \frac{k_B T}{\sqrt{2}\pi \delta_m^2 p}, \tag{2}$$

where δ_m is the effective radius of gas molecules, m; K_B is the Boltzmann constant. Average molecular free path increases with the increase of temperature, but the trend is not sensitive and only plays a slight role when pressure is lower than 1 MPa. The change of pressure has a great influence on this value, and the molecular average free path will gradually increase with the decrease of pressure, and the increasing range will become larger. For specific scale reservoir pores, the reservoir temperature can be regarded as a fixed value, but the decrease of reservoir pressure will increase the Knudsen number rapidly, leading to the variation of gas flow mechanism. Therefore, a single flow mechanism equation is not suitable for unconventional gas reservoir development. Moreover, the pore types of nanopores are complex, and the study of nanopores alone cannot meet the actual needs. It is urgent to establish a high-precision cross-scale gas bulk transport equation suitable for different cross-sections. Next, bulk-gas transport equations of circular tube holes and slit holes in different Knudsen number ranges are introduced.

2.1. Cylindrical Nanopore. When $Kn < 0.001$, the gas nanopore transport mechanism is continuous flow, and the intermolecular collision dominates the transport process. At this time, the flow characteristics can be characterized by the nonslip Navier-Stokes equation [35].

$$J_{yc} = -\frac{r^2 p}{8\mu_g RT}\frac{dp}{dl}, \quad (3)$$

where J_{yc} represents the continuous flow transmission capacity, mol/(m^2·s); r is the pore radius of porous medium, m; p is the fluid flow pressure, Pa; μ_g is the gas viscosity, Pa ·s; R is the general gas constant, J/(mol·K); T is the temperature of the fluid, K; and l is the distance in the gas flow direction, m.

When the Knudsen number is between 0.001 and 0.1, the gas nanopore transmission mechanism is slippage flow, the collision frequency between gas molecules and wall increases gradually, and the nonslippage condition breaks down. Then, it is found that satisfactory results can be obtained by modifying the slip boundary conditions [36–46].

$$J_{ys} = -\frac{r^2 p}{8\mu_g RT}\left(1 + \frac{4Kn}{1 - bKn}\right)\frac{dp}{dl}. \quad (4)$$

Among them, J_{ys} characterizing the slippage flow transmission capacity of gas circular tube hole, mol/(m^2·s); b is the gas slippage constant. When the value is 0, it represents the first-order slippage condition, and when the value is -1, it represents the second-order slippage condition. Moreover, according to a large number of molecular simulation and experimental data, the fitting effect of the second-order slippage condition is obviously better than that of the first-order, so the expression of nanopore phase transport of gas slippage flow can be simplified as follows:

$$J_{ys} = -\frac{r^2 p}{8\mu_g RT}\left(1 + \frac{4Kn}{1 + Kn}\right)\frac{dp}{dl}. \quad (5)$$

When the Knudsen number is greater than 10, the transmission mechanism of gas nanopores is Knudsen diffusion, the collision frequency between gas molecules continues to decline, and the collision frequency between molecules and wall dominates the transmission process, which can be expressed by Knudsen equation [16, 26, 27].

$$J_{yk} = -\frac{d}{3}\sqrt{\frac{8}{\boldsymbol{\pi RTM}}}\frac{dp}{dl}. \quad (6)$$

In view of the dominant collision between gas molecules and wall, the influence of wall roughness on gas diffusion must be considered. The coarser the wall, the weaker the gas diffusion ability. The specific relationship can be characterized by the following formula [17, 27].

$$J_{yk} = -\frac{d}{3}\delta^{D_f - 2}\sqrt{\frac{8}{\boldsymbol{\pi RTM}}}\frac{dp}{dl}, \quad (7)$$

where δ is the ratio of molecular diameter to local pore diameter, dimensionless; D_f is the fractal dimension of pore wall, dimensionless. When the fractal dimension is 2, it represents a smooth wall and has no effect on the gas transmission capacity; when the fractal dimension is 3, it represents a rough wall.

2.2. Slit Nanopores. In order to facilitate the investigation of pore morphology on gas transmission capacity, the aspect ratio is defined here (AR*).*

$$\mathrm{AR} = \frac{w}{h}, \quad (8)$$

where w is the width of slit hole, m; h is the height of slit hole, m.

When the Knudsen number is less than 0.001, the flow velocity of gas molecules on the wall is zero, which is a continuous flow. The specific expression can be seen from Hagen Poiseuille [47].

$$J_{xc} = C(\mathrm{AR})\frac{wh^3}{12\mu}\frac{p}{RT}\frac{dp}{dl}, \quad (9)$$

where J_{xc} is the characterization of gas slippage flow transport capacity in slit holes, mol/s; $C(\mathrm{AR})$ is the continuous flow correction coefficient of slit holes with different aspect ratios, dimensionless [26, 48].

$$C(\mathrm{AR}) = 1 - \frac{192}{\mathrm{AR}\pi^5}\sum_{i=1,3,5\cdots}^{\infty}\frac{\tanh\left(\boldsymbol{i\pi AR}/2\right)}{i^5}. \quad (10)$$

When the Knudsen number is between 0.001 and 0.1, the collision between gas and wall cannot be ignored. After a large number of molecular simulation and experimental results, for the slippage flow, the second-order slippage boundary condition is more reasonable than the first-order boundary slippage condition. At this time, the expression of gas slippage flow is provided.

$$J_{xs} = C(\mathrm{AR})\frac{wh^3}{12\mu}\frac{p}{RT}\left(1 + \frac{6Kn}{1 + Kn}\right)\frac{dp}{dl}, \quad (11)$$

where J_{xs} represents the gas slippage flow transmission capacity of slit hole, mol/s.

When the Knudsen number is greater than 10, the transmission mechanism of gas slit hole is Knudsen diffusion, and the collision frequency between molecules and wall dominates the transmission process. Considering the influence of cross-section shape, the Knudsen diffusion transmission capacity of gas bulk phase in slit hole can be expressed [26].

$$\begin{aligned} J_{xk} &= B(\mathrm{AR})\frac{wh^2}{\sqrt{2RTM}}\frac{dp}{dl}, \\ B(\mathrm{AR}) &= \left[\mathrm{AR}^2 \ln\left(\frac{1}{\mathrm{AR}} + \sqrt{1 + \frac{1}{\mathrm{AR}^2}}\right)\right. \\ &\quad \left. + \mathrm{AR}\ln\left(\mathrm{AR} + \sqrt{1 + \mathrm{AR}^2}\right) - \frac{\left(\mathrm{AR}^2 + 1\right)^{1.5}}{3} + \frac{1 + \mathrm{AR}^3}{3}\right], \end{aligned} \quad (12)$$

where $B(\mathrm{AR})$ is the Knudsen diffusion correction coefficient of slit holes with different aspect ratios, dimensionless. It can be seen from the expression that this value is only affected by the aspect ratio.

3. Model Establishment and Verification

3.1. Cylindrical Nanopores. Comprehensive analysis of the comparison results between existing models and molecular simulation shows that the majority of existing models are quite different from molecular simulation results, and only Wu's model and Knudsen's model perform well. Among them, the calculation results of Wu's model are consistent with the molecular simulation data in the slippage flow domain, but there are large errors in the transition flow stage, which cannot accurately describe the gas bulk phase transmission capacity of the transition flow. Knudsen's model is consistent with the molecular simulation results at high Knudsen number stage, but it will overestimate the bulk phase transport capacity of slipstream gas. Referring to Wu's model which can accurately describe the slippage flow and Knudsen's model which can accurately describe the stage of high Knudsen number, the weight factors of slippage flow and Knudsen diffusion are obtained, respectively. Coupling the mentioned two mechanisms, a nanoscale bulk-gas transport model in cylindrical pores, suitable for all Knudsen number, is obtained. The corresponding expression is given below.

$$\begin{gathered}
J_{ya} = \frac{1}{1+5Kn} J_{ys} + \frac{Kn+2.507}{Kn+3.095} J_{yk}, \\
\frac{J_{ya}}{J_{yk}} = \frac{3\pi}{128\delta^{D_f-2}Kn}\left(1+\frac{4Kn}{1+Kn}\right)\frac{1}{1+5Kn} + \frac{Kn+2.507}{Kn+3.095}, \\
\frac{J_{ya}}{J_{yc}} = \left(1+\frac{4Kn}{1+Kn}\right)\frac{1}{1+5Kn} + \frac{\delta^{D_f-2}(Kn+2.507)Kn}{Kn+3.095}\frac{128}{3\pi}.
\end{gathered} \tag{13}$$

The proposed bulk-gas transport model without fitting parameters can accurately describe the characteristics of each flow mechanism. When the Knudsen number is extremely small, it will degenerate into a continuous flow equation according to formula (4), which is much greater than that at low Knudsen number, so formula (29) will degenerate into a continuous flow equation at low Knudsen number. When the Knudsen number is maximum, it can be directly reduced to Knudsen diffusion equation according to formula (29). When the flow mechanism is slippage flow and transition flow, it can be verified by comparing the calculated values of the model in this paper with the molecular simulation results. The specific comparison results are shown in Figures 1 and 2.

Through the analysis of Figures 1 and 2, it can be seen that the nanopore phase transport model proposed in this paper can always maintain very high accuracy within the whole Knudsen range. Only when the Knudsen number is near 1, the gas transport capacity is slightly underestimated, but its accuracy is still higher than that of Knudsen model. So far, the reliability of the proposed bulk phase transport model without fitting parameters for all Knudsen numbers has been verified, and its high-precision characteristics are shown by comparison with Wu model and Knudsen model.

3.2. Slit Nanopores. Based on the proposed nonfitting parameter nanotube bulk phase transport model and referring to its basic form of weight factor, the slip flow equation and Knudsen diffusion equation applicable to slit hole are coupled, that is, formula (10) and formula (11), and the nonfitting parameter slit hole bulk phase transport model is established. The specific expression is as follows:

$$\begin{gathered}
J_{xa} = \frac{1}{1+6Kn} J_{xs} + \frac{Kn+2.45}{Kn+3.6} J_{xk}, \\
\frac{J_{xa}}{J_{xk}} = \frac{C(\mathrm{AR})}{6Kn}\left(1+\frac{6Kn}{1+Kn}\right)\frac{1}{1+6Kn} + \frac{Kn+2.45}{Kn+3.6}B(\mathrm{AR}), \\
\frac{J_{xa}}{J_{xc}} = \left(1+\frac{6Kn}{1+Kn}\right)\frac{C(\mathrm{AR})}{1+6Kn} + B(\mathrm{AR})\frac{Kn+2.45}{Kn+3.6}6Kn.
\end{gathered} \tag{14}$$

Similarly, when the Knudsen number is extremely high, the slit hole model, i.e., formula (32), can be reduced to Knudsen diffusion equation, and when the Knudsen number is extremely small, the model can be reduced to continuity equation. In order to verify the accuracy of the proposed nonfitting parameter model for the transmission capacity of different slit holes and its reliability in the stage of slippage flow and transition flow, the gas bulk phase transmission capacity of different aspect ratios (1, 2, and 4) in different Knudsen number ranges is calculated by the model, and the results are compared with the molecular simulation data [32].

By analyzing the comparison results of Figures 3 and 4, it can be seen that the calculation results of the volume phase transmission capacity of the slit pore model proposed in this paper for different forms of pores within the whole Knudsen range are always highly consistent with the molecular simulation data. At low Knudsen number, only when the aspect ratio is 2, there is a slight difference. At high Knudsen number, calculation results for the transmission capacity of different pore shape can always be consistent with the molecular simulation data. Therefore, the reliability and high-precision characteristics of the slit pore model are verified by comparison with the molecular simulation.

So far, the fitting parameter free circular hole model and slit hole model suitable for the whole Knudsen number range have been established for the first time, and their reliability and accuracy have been verified by comparing with molecular simulation results and existing models. Because the established circular hole and slit hole models do not contain fitting parameters and are suitable for the full Knudsen number with high accuracy, they show the practicability and simplicity that other models do not have. Next, the proposed model is used to study the effects of pore morphology (cylindrical nanopores and slit nanopores), pore scale, and reservoir pressure on gas bulk phase transmission capacity in

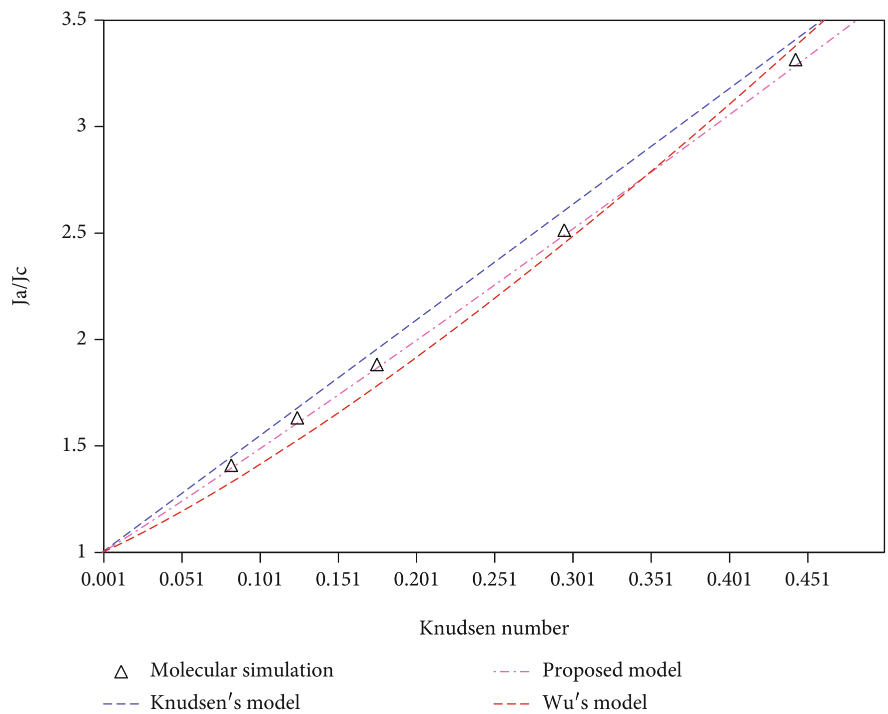

Figure 1: Comparison between proposed model and molecular simulation with low Kn.

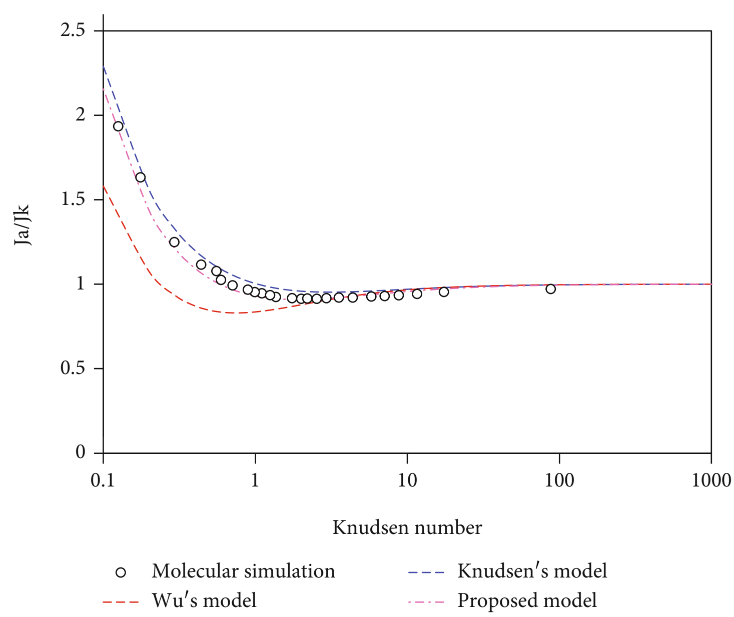

Figure 2: Comparison between proposed model and molecular simulation with high Kn.

the process of gas reservoir development, and the transmission contribution of each transmission mechanism is quantitatively analyzed.

4. Results and Discussion

In the conventional reservoir, because it does not contain a large number of nanopores and the formation pressure is high, the reservoir flow mechanism will not change in the whole life production cycle of the gas well, and it is always continuous flow. In this case, the bulk phase transmission capacity is close to a constant. However, for coal and shale reservoirs with diverse nanopores, with the development, the reservoir pressure continues to decrease, and different production stages often correspond to different transmission types, so the nanopore phase transmission capacity will change greatly. Studying the gas transmission capacity of reservoirs in different production stages is helpful to formulate a reasonable gas production scheme and provide constructive suggestions for the formulation of gas reservoir development scheme. Assuming that the

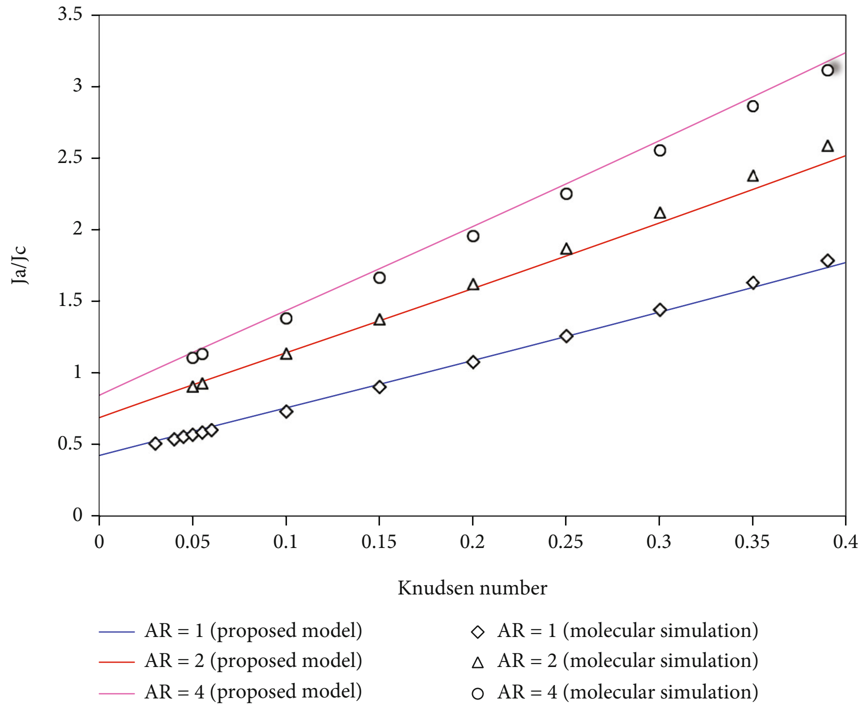

Figure 3: Comparison between proposed model and molecular simulation with low Kn.

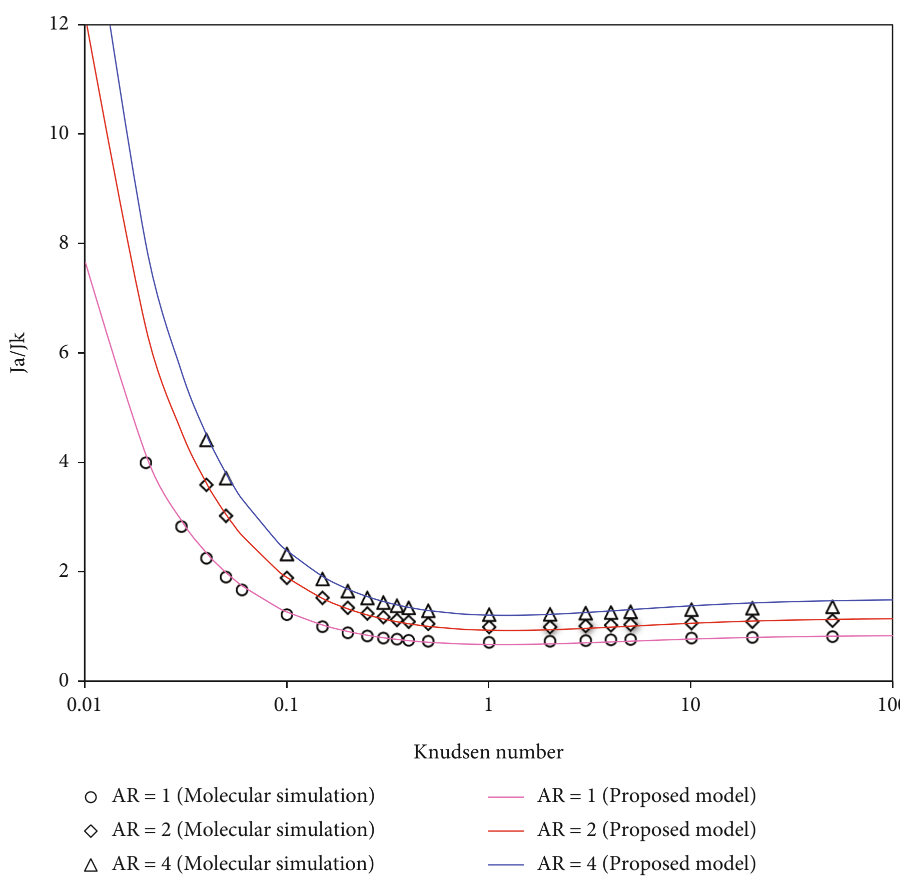

Figure 4: Comparison between proposed model and molecular simulation with high Kn.

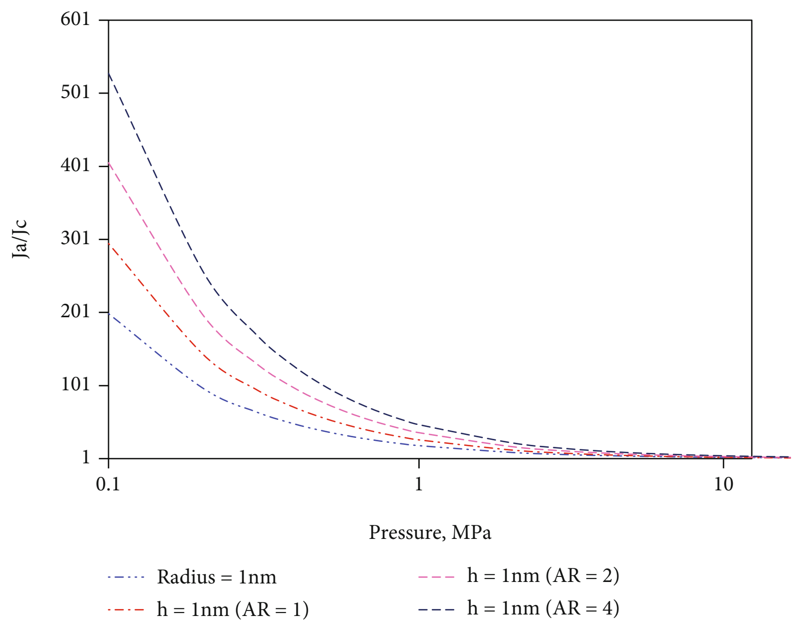

FIGURE 5: Gas transport capacity versus pressure with different cross-section shapes.

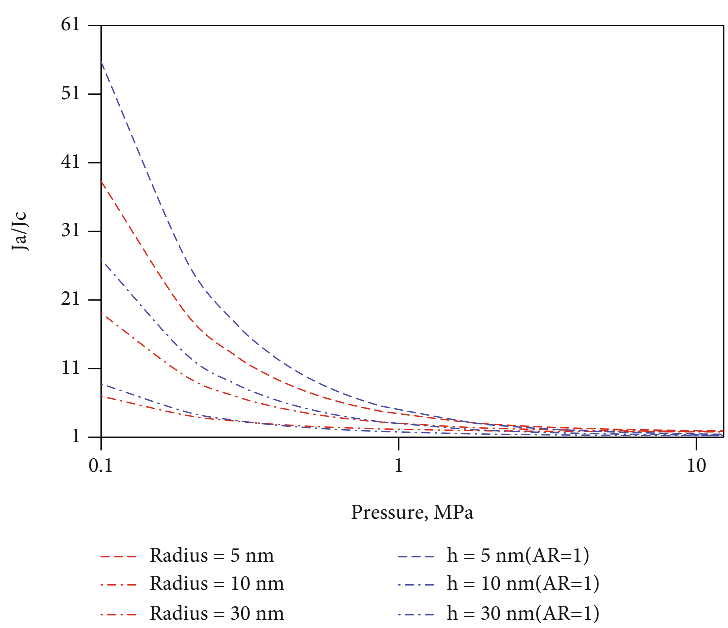

FIGURE 6: Effect of pore size on gas transport capacity.

reservoir temperature is 323 K, and taking methane as an example, the gas bulk phase transmission capacity in pores with different scales (1~50 nm) is calculated and analyzed, respectively. In view of the characterization of the continuous flow transmission capacity, which remains unchanged under the total Knudsen number, the change of nanopore transmission capacity with pressure is described by the change relationship with reservoir pressure.

According to the analysis of Figure 5, for the specific pore scale, the bulk-gas transport capacity shows an upward trend with the decrease of reservoir pressure. When the reservoir pressure is greater than 1 MPa, the bulk-gas transmission capacity of all pores increases slowly. When the reservoir pressure is less than 1 MPa, the bulk phase transmission capacity of pores increases rapidly, and the growth range increases with the decrease of pressure. For different forms of pores, at the same scale, the transmission capacity of slit nanopores is significantly higher than that of cylindrical nanopores, and transmission capacity of slit nanopores will increase with the increase of aspect ratio. In Figure 6, it can be seen that whether for circular pores or slit pores, under the same reservoir pressure, their bulk phase transmission capacity increases with the decrease of scale, and the growth range increases with the decrease of scale. It can also be seen from Figure 6 that although the transmission capacity of slit holes is stronger than that of cylindrical

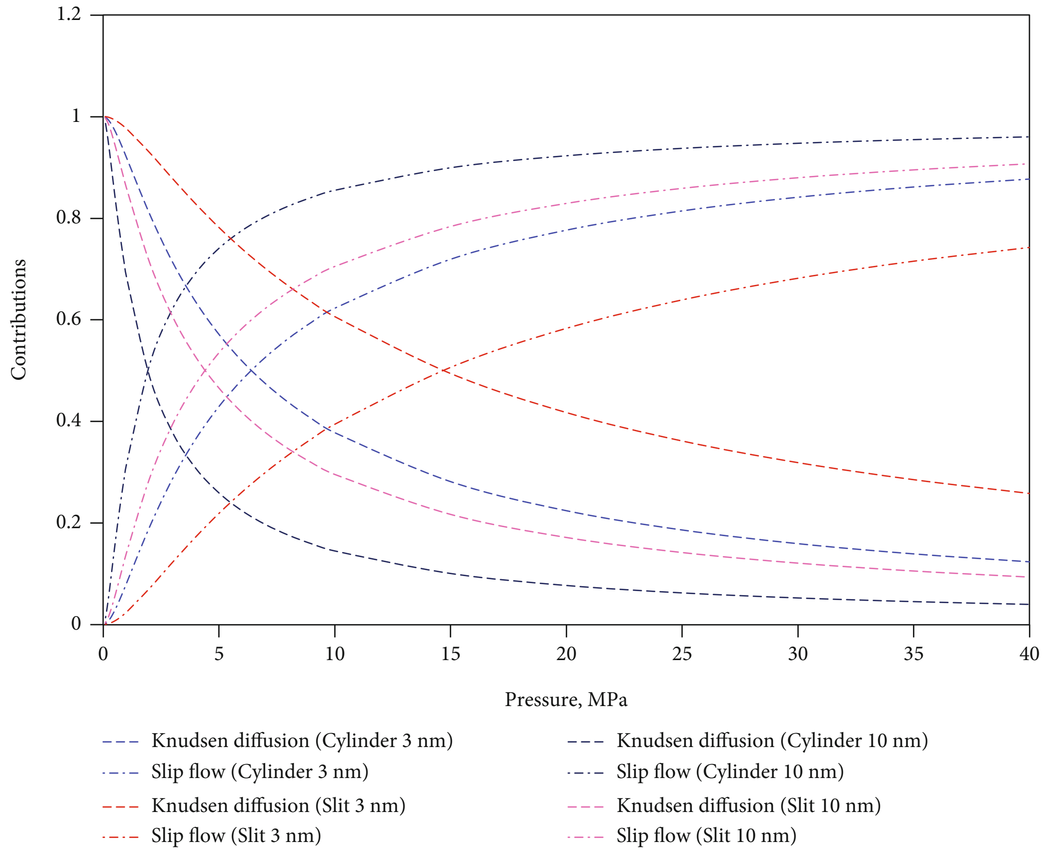

Figure 7: Contribution of different gas transport mechanisms.

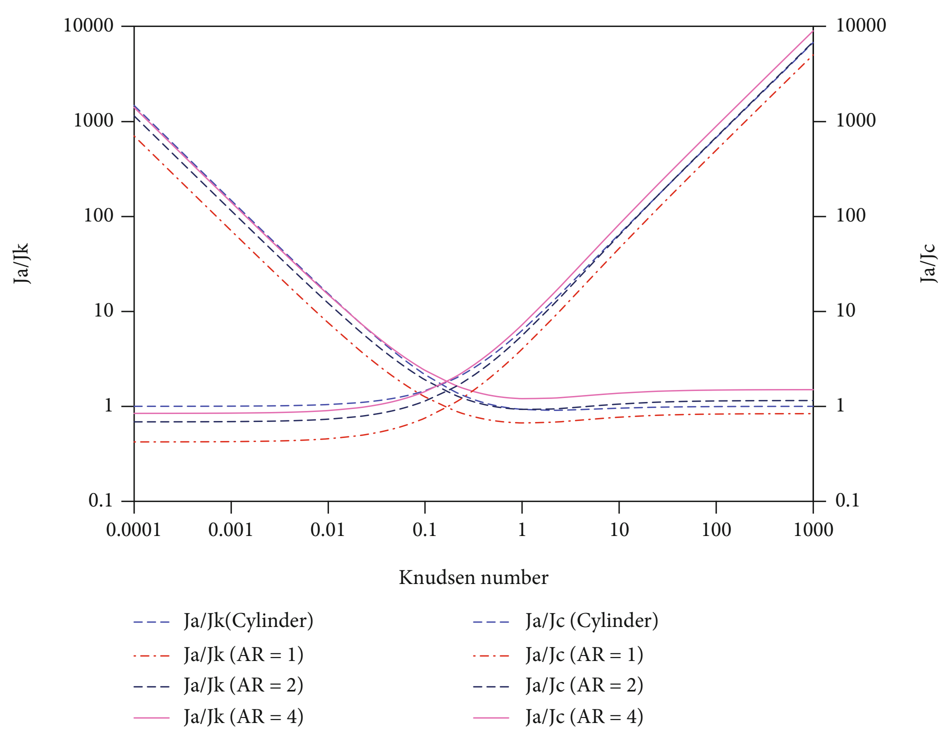

Figure 8: The bulk-gas transport capacity with different Kn values.

nanopores at the same pore size, both differences will gradually become narrow with the increase of pore scale. Therefore, when the pore size in the reservoir is greater than 30 nm, the bulk phase transmission capacity of circular pore and slit pore is basically the same. When the pore size in the reservoir is less than 30 nm, we should focus on the influence of pore morphology on the transmission capacity.

The models, suitable for cylindrical nanopores and slit nanopores, proposed in this paper are obtained by giving the expression of weight factor and coupling slippage flow and Knudsen diffusion. With the development of shale gas, the reservoir pressure decreases continuously, and the contribution of slippage flow and Knudsen diffusion to the overall transmission capacity will change. Here, the contribution factors of slippage flow and Knudsen diffusion to gas bulk phase transmission capacity are defined as follows.

$$\begin{aligned}
F_{yk} &= \frac{1}{(1/1+5Kn)(Kn+3.095/Kn+2.507)J_{ys}/J_{yk}+1},\\
F_{ys} &= \frac{1}{1+(1+5Kn)(Kn+2.507/Kn+3.09)J_{yk}/J_{ys}},\\
F_{xk} &= \frac{1}{(1/1+6Kn)(Kn+3.6/Kn+2.45)J_{xs}/J_{xk}+1},\\
F_{xs} &= \frac{1}{1+(1+6Kn)(Kn+2.45/Kn+3.6)J_{xk}/J_{xs}}.
\end{aligned} \tag{15}$$

It can be seen from Figure 7 that for pores of the same size and shape, with the increase of reservoir pressure, contribution of slippage flow gradually increases and the contribution of Knudsen diffusion gradually decreases. This is because the increase of pressure reduces the molecular average free path and Knudsen number, and the flow mechanism in pores changes from Knudsen diffusion to slippage flow. For the pores with the same size and different shapes, with the development, the contribution of Knudsen diffusion in the slit nanopores is always higher than that in the circular nanopores. For the same shape and different pore-scale pores, the analysis shows that the contribution of slippage flow in large-scale pores is higher than that in small pores. Through the analysis of Figure 7, it can also be seen that for the nanoscale pores analyzed in the figure, when the reservoir pressure is higher than 10 MPa, the transmission contribution of each transmission mechanism changes slowly, while when the reservoir pressure is lower than 10 MPa, the transmission mechanism changes sharply. It shows that in the actual gas reservoir production process, due to the concept of pressure drop funnel, there is a large pressure difference between the near well zone and the far well zone. The near well area is mainly affected by Knudsen diffusion, and the far well area is mainly affected by slippage flow mechanism.

Through the established models, the bulk phase transmission capacity of different forms of pores in the whole Knudsen number range is analyzed. It can be seen from the comparison in Figure 8 that for slit nanopores, the larger the aspect ratio of pores, the stronger the bulk phase transmission capacity. The transmission capacity of slit nanopores with AR = 4 is about 1.23 and 2 times that of slit nanopores with AR = 2 and AR = 1 in the whole Knudsen range. For the transmission capacity in cylindrical nanopores, when the Knudsen number is less than 0.1, its transmission capacity is higher than all slit nanopores. When the Knudsen number is between 0.1~10, the transmission capacity in cylindrical nanopores is lower than the slit hole transmission capacity of AR = 4. When the Knudsen number is greater than 10, the transmission capacity in cylindrical nanopores is lower than that in slit nanopores of AR = 2 and only higher than the slit hole with AR = 1.

5. Conclusions

(1) By fully comparing and analyzing the existing models and molecular simulation results, it is found that Wu's model has high accuracy in the slippage flow stage, and Knudsen's model is consistent with the molecular simulation results in the high Knudsen number stage. Using Wu's model and Knudsen's model for reference, the weight factors of slippage flow and Knudsen diffusion are obtained, respectively. The two mechanisms are coupled to obtain the nonfitting parameter bulk-gas transport model. According to the model for cylindrical nanopores, corresponding weight factors are modified to obtain the nonfitting parameter for slit nanopores

(2) Under the same reservoir pressure, the bulk-gas transmission capacity of cylindrical nanopores and slit nanopores increases with the decrease of pore size. For different forms of pores, at the same scale, the transmission capacity of slit nanopores is significantly higher than that of cylindrical nanopores, and the transmission capacity of slit nanopores will increase with the increase of aspect ratio, but the difference between the two will gradually narrow with the increase of pore size. When the pore size in the reservoir is greater than 30 nm, bulk-gas transmission capacity of cylindrical and slit nanopores is basically the same

(3) For slit nanopores, the larger the aspect ratio of pores, the stronger the bulk-gas transmission capacity. The transmission capacity of slit nanopores with AR = 4 is about 1.23 and 2 times that of slit pores with AR = 2 and AR = 1 in the whole Knudsen number range. For transmission capacity in cylindrical nanopores, when the Knudsen number is less than 0.1, its transmission capacity is higher than all slit nanopores analyzed in the calculation case. When Knudsen number is between 0.1~10, transmission capacity in cylindrical nanopores is lower than the slit nanopores of AR = 4. When Knudsen number is greater than 10, transmission capacity in cylindrical nanopores is lower than that of slit nanopores of AR = 2 and only higher than the slit nanopores with AR = 1

Data Availability

Data is available on request.

Ethical Approval

On behalf of all the coauthors, the corresponding author states that there are no ethical statements contained in the manuscripts.

Conflicts of Interest

The author declares that there is no conflict of interest regarding the publication of this paper.

Acknowledgments

The research acknowledges the financial support of the Zunyi Normal University (BS- [2019]-20).

References

[1] C. Rühl and J. Giljum, "BP global energy outlook 2030," *Voprosy Ekonomiki*, no. 5, pp. 109–128, 2013.

[2] M. Yoshimune, T. Yamamoto, M. Nakaiwa, and K. Haraya, "Preparation of highly mesoporous carbon membranes via a sol-gel process using resorcinol and formaldehyde," *Carbon*, vol. 46, no. 7, pp. 1031–1036, 2008.

[3] C. Özgen Karacan, "Heterogeneous sorption and swelling in a confined and stressed coal during CO_2 injection," *Energy & Fuels: An American Chemical Society Journal*, vol. 17, no. 6, pp. 1595–1608, 2003.

[4] H. Siriwardane, I. Haljasmaa, and R. Mclendon, "Influence of carbon dioxide on coal permeability determined by pressure transient methods," *International Journal of Coal Geology*, vol. 77, no. 1–2, pp. 109–118, 2009.

[5] J. J. Howard, "Porosimetry measurement of shale fabric and its relationship to illite/smectite diagenesis," *Clays and Clay Minerals*, vol. 39, no. 4, pp. 355–361, 1991.

[6] P. H. Nelson, "Pore-throat sizes in sandstones, tight sandstones, and shales," *AAPG Bulletin*, vol. 93, no. 3, pp. 329–340, 2009.

[7] C. Cercignani and A. Daneri, "Flow of a rarefied gas between two parallel plates," *Journal of Applied Physics*, vol. 34, no. 12, pp. 3509–3513, 1963.

[8] S. Roy, R. Raju, H. F. Chuang, B. A. Cruden, and M. Meyyappan, "Modeling gas flow through microchannels and nanopores," *Journal of Applied Physics*, vol. 93, no. 8, pp. 4870–4879, 2003.

[9] K. Wu, Z. Chen, and H. Wang, *A Model for Real Gas Transfer in Nanopores of Shale Gas Reservoirs*, EUROPEC, Madrid, Spain, 2015.

[10] E. Piekos and K. Breuer, "DSMC modeling of micromechanical devices," in *30th Thermophysics Conference*, 1995.

[11] G. A. Bird, *Molecular Gas Dynamics and the Direct Simulation of Gas Flows*, , location is USA, 1998Clarendon Press, Oxford, 1998.

[12] M. L. Hudson and T. J. Bartel, *DSMC Simulation of Thermal Transpiration and Accommodation Pump*, Rarefied Gas Dynamics, 1999.

[13] D. C. Rapaport, *The Art of Molecular Dynamics Simulation*, Cambridge University Press, 2011.

[14] S. K. Loyalka and S. A. Hamoodi, "Poiseuille flow of a rarefied gas in a cylindrical tube: solution of linearized Boltzmann equation," *Physics of Fluids A: Fluid Dynamics*, vol. 2, no. 11, pp. 2061–2065, 1990.

[15] F. Javadpour, D. Fisher, and M. Unsworth, "Nanoscale gas flow in shale gas sediments," *Journal of Canadian Petroleum Technology*, vol. 46, no. 10, pp. 55–61, 2007.

[16] F. Javadpour, "Nanopores and apparent permeability of gas flow in mudrocks (shales and siltstone)," *Journal of Canadian Petroleum Technology*, vol. 48, no. 8, pp. 16–21, 2009.

[17] Z. Sun, B. Huang, Y. Li, H. Lin, S. Shi, and W. Yu, "Nanoconfined methane flow behavior through realistic organic shale matrix under displacement pressure: a molecular simulation investigation," *Journal of Petroleum Exploration and Production Technology*, vol. 12, no. 4, pp. 1193–1201, 2022.

[18] H. Adzumi, "Studies on the flow of gaseous mixtures through capillaries. I the viscosity of binary gaseous mixtures," *Bulletin of the Chemical Society of Japan*, vol. 12, no. 5, pp. 199–226, 1937.

[19] H. Adzumi, "Studies on the flow of gaseous mixtures through capillaries. II. The molecular flow of gaseous mixtures," *Bulletin of the Chemical Society of Japan*, vol. 12, no. 6, pp. 285–291, 1937.

[20] H. Adzumi, "Studies on the flow of gaseous mixtures through capillaries. III. The flow of gaseous mixtures at medium pressures," *Bulletin of the Chemical Society of Japan*, vol. 12, no. 6, pp. 292–303, 1937.

[21] Q. Liu, P. Shen, and P. Yang, *Pore scale network modelling of gas slippage in tight porous media*, Fluid Flow & Transport in Porous Media Mathematical & Numerical Treatment, 2002.

[22] K. G. R. Ertekin and F. C. Schwerer, "Dynamic gas slippage: a unique dual-mechanism approach to the flow of gas in tight formations," *SPE Formation Evaluation*, vol. 1, no. 1, pp. 43–52, 1986.

[23] P. N. Azom and F. Javadpour, "Dual-continuum modeling of shale and Tight Gas Reservoirs," in SPE Annual Technical Conference and Exhibition, San Antonio, Texas, USA, 2012.

[24] H. Singh, F. Javadpour, A. Ettehadtavakkol, and H. Darabi, "Nonempirical apparent permeability of shale," *SPE Reservoir Evaluation & Engineering*, vol. 17, no. 3, pp. 414–424, 2014.

[25] R. F. Aguilera, J. F. Ramirez, and C. E. Ortega, *A Variable Shape Distribution (VSD) Model for Characterization of Pore Throat Apertures and Drill Cuttings in Tight and Shale Reservoirs*, 2012.

[26] A. Beskok and G. E. Karniadakis, "Report: a model for flows in channels, pipes, and DUCTS at micro and NANO scales," *Nanoscale and Microscale Thermophysical Engineering*, vol. 3, no. 1, pp. 43–77, 1999.

[27] W. Keliu and L. Xiangfang, "Real gas transport through nanopores of shale gas reservoirs," *China Science: Science and technology*, vol. 46, no. 1, pp. 68–78, 2016.

[28] M. R. R. Shahri, R. Aguilera, and A. Kantzas, "A new unified diffusion-viscous flow model based on pore level studies of tight gas formations," *SPE Journal*, vol. 18, no. 1, pp. 38–49, 2012.

[29] J. Liming, Q. Junli, and X. Yanqing, "SEM micropore characteristics and methane adsorption of common clay minerals," *Journal of Petroleum*, vol. 33, no. 2, pp. 249–256, 2012.

[30] R. Aringhieri, “Nanoporosity characteristics of some natural clay minerals and soils,” *Clays and Clay Minerals*, vol. 52, no. 6, pp. 700–704, 2004.

[31] D. J. K. Ross and R. M. Bustin, “The importance of shale composition and pore structure upon gas storage potential of shale gas reservoirs,” *Marine and Petroleum Geology*, vol. 26, no. 6, pp. 916–927, 2009.

[32] S. Takata and H. Funagane, “Poiseuille and thermal transpiration flows of a highly rarefied gas: over-concentration in the velocity distribution function,” *Journal of Fluid Mechanics*, vol. 669, no. 1, pp. 242–259, 2011.

[33] M. Knudsen, “Die Gesetze der Molekularströmung und der inneren Reibungsströmung der Gase durch Röhren,” *Annalen der Physik*, vol. 333, no. 1, pp. 75–130, 1909.

[34] S. A. Schaaf and P. L. Chambré, *Flow of Rarefied Gases*, Princeton University Press, 1961.

[35] J.-G. Choi, D. D. Do, and H. D. Do, “Surface diffusion of adsorbed molecules in porous media: monolayer, multilayer, and capillary condensation regimes,” *Industrial & Engineering Chemistry Research*, vol. 40, no. 19, pp. 4005–4031, 2001.

[36] E. H. Kennard, *Kinetic theory of gases*McGraw-Hill, New York, 1st ed edition.

[37] W. A. Ebert and E. M. Sparrow, “Slip flow in rectangular and annular Ducts,” *Journal of Fluids Engineering*, vol. 87, no. 4, pp. 1018–1024, 1965.

[38] H. Deng, G. Sheng, H. Zhao et al., “Integrated optimization of fracture parameters for subdivision cutting fractured horizontal wells in shale oil reservoirs,” *Journal of Petroleum Science and Engineering*, vol. 212, p. 110205, 2022.

[39] A. K. Sreekanth, “Slip flow through long circular tubes,” in *Proceedings of the 6th international symposium on rarefied gas dynamic*, pp. 667–680, 1969.

[40] G. Sheng, Y. Su, and W. Wang, “A new fractal approach for describing induced-fracture porosity/permeability/ compressibility in stimulated unconventional reservoirs,” *Journal of Petroleum Science and Engineering*, vol. 179, pp. 855–866, 2019.

[41] S. Chapman and T. G. Cowling, *The Mathematical Theory of Non-uniform Gases*, Cambrige University Press, Cambrige, 1952.

[42] G. E. Karniadakis and A. Bekok, *Microflows: Fundamentals and Simulation*, Springer, Berlin Heidelberg New York, 2002.

[43] Z. Sun, B. Huang, K. Wu et al., “Nanoconfined methane density over pressure and temperature: wettability effect,” *Journal of Natural Gas Science and Engineering*, vol. 99, article 104426, 2022.

[44] Y. Mitsuya, “Modified Reynolds equation for ultra-thin film gas lubrication using 1.5Order slip-flow model and considering surface accommodation coefficient,” *Transactions of the Japan Society of Mechanical Engineers C*, vol. 115, no. 2, pp. 289–294, 1993.

[45] J. Maurer, P. Tabeling, P. Joseph, and H. Willaime, “Second-order slip laws in microchannels for helium and nitrogen,” *Physics of Fluids*, vol. 15, no. 9, pp. 2613–2621, 2003.

[46] Z. Sun, B. Huang, Y. Liu et al., “Gas-phase production equation for CBM reservoirs: interaction between hydraulic fracturing and coal orthotropic feature,” *Journal of Petroleum Science and Engineering*, vol. 213, article 110428, 2022.

[47] Z. Sun, S. Wang, H. Xiong, K. Wu, and J. Shi, “Optimal nanocone geometry for water flow,” *AICHE Journal*, vol. 68, no. 3, article e17543, 2022.

[48] S. S. Antman, J. E. Marsden, and L. Sirovich, *Microflows and Nanoflows*, Springer, 2005.